

# Network induces burst synchronisation in cat brain

Ewandson L. Lameu<sup>1</sup>, Fernando S. Borges<sup>1</sup>, Rafael R. Borges<sup>1</sup>, Antonio M. Batista<sup>1,2,\*</sup>, Murilo S. Baptista<sup>3</sup>, Ricardo L. Viana<sup>4</sup>

<sup>1</sup>*Pós-Graduação em Ciências/Física, Universidade Estadual de Ponta Grossa, 84030-900, Ponta Grossa, PR, Brazil.*

<sup>2</sup>*Departamento de Matemática e Estatística, Universidade Estadual de Ponta Grossa, 84030-900, Ponta Grossa, PR, Brazil.*

<sup>3</sup>*Institute for Complex Systems and Mathematical Biology, University of Aberdeen, AB24 3UE, Aberdeen, SUPA, UK.*

<sup>4</sup>*Departamento de Física, Universidade Federal do Paraná, 81531-990, Curitiba, PR, Brazil.*

---

## Abstract

The brain of mammals are divided into different cortical areas that are anatomically connected forming larger networks which perform cognitive tasks. The cat cerebral cortex is composed of 65 areas organised into the visual, auditory, somatosensory-motor and frontolimbic cognitive regions. We have built a network of networks, in which networks are connected among themselves according to the connections observed in the cat cortical areas aiming to study how inputs drive the synchronous behaviour in this cat brain-like network. We show that without external perturbations it is possible to observe high level of bursting synchronisation between neurons within almost all areas, except for the auditory area. Bursting synchronisation appears between neurons in the auditory region when an external perturbation is applied in another cognitive area. This is a clear evidence that pattern formation and collective behaviour in the brain might be a process mediated by other brain areas under stimulation.

*Keywords:* synchronisation, bursting neurons, network

---

---

\*Corresponding author: antoniomarcosbatista@gmail.com

## 1. Introduction

The nervous system of mammals is responsible for collecting and processing information, where the signals are sent by neurons [1]. The propagation of neural signals occurs through electrical and chemical synapses, as a result of the difference in electric potential between the exterior and the interior of a neuron [2]. Neurons connect to each other forming complex layered structures [3]. The different cortical layers have particular distributions of neuronal cell types, as well as connections with other cortical and sub-cortical regions [4]. The mammalian brain is composed of distinct areas, the cerebellar cortex, and non-cortical nuclei. The cortex presents fundamental divisions such as the hippocampus formation, the olfactory cortex, and associated areas [5].

In this work we consider the cat cerebral cortex. Scannell and collaborators [6, 7] have relevant results related to the cortical system of the cat. They showed the connection organisation, and reported that there are 1139 corticocortical connections among 65 cortical areas. The cortical areas are organised into four connectional clusters, corresponding to visual, auditory, somatosensory-motor, and frontolimbic areas [8].

Here we focus on dynamical features such as bursting synchronisation and desynchronisation [9]. Bursting synchronisation are thought to play relevant roles in information binding in the mammalian brain [10]. However, bursting synchronisation may be associated with pathologies like seizures [11] or Parkinson's disease [12]. For this reason, studies about synchronisation are of great interest to neuroscience.

Our purpose in this work is to study the formation of patterns of synchronisation and desynchronisation in a neural network model of the cat brain, using the matrix of corticocortical connections in the cat [7]. The matrix represents the densities of connections in 65 cortical areas is on undirected weighted adjacency. We describe each cortical area as a small-world network [13, 14, 15]. Small-world networks have been proposed to be an efficient solution for achieving phase synchronisation of bursting neurons [16]. In addition they have been found to be linked to different levels of models of the brain.

Small-world networks have been intensively investigated in computational neuroscience [17]. The characterisation can be made on two basic levels: a microscopic, neuroanatomic level, and a macroscopic, functional level. Studies at the former level are limited to those few examples in which there is available data on the neuronal connectivity, as the worm *C. Elegans*, which is considered one of the simplest and most primitive organisms that shares

essential biological characteristics of the more complex species [18]. Moreover, there have been studies of large-scale anatomical connection patterns of the human cortex using cortical thickness measurements from magnetic resonance imaging [19]. The human brain anatomical network at this level has an average path length and a clustering coefficient with values presented by networks with small-world property. Stam and collaborators, in a study of functional brain networks, observed that there is a loss of small-world network characteristics in patients with Alzheimer’s disease, in particular with an increase of the average path length with no significant changes in the clustering coefficient [20].

At the macroscopic level of description of neural networks, the use of non-invasive techniques as electroencephalography, functional magnetic resonance imaging and magnetoencephalography provides anatomical and functional connectivity patterns between different brain areas [21, 22]. This information provides a way to study the brain cortex, considering the latter as being divided into anatomic and functional areas, linked by axonal fibers. Scannell and coworkers have investigated the anatomical connectivity matrix of the visual cortex for the macaque monkey and the cat [6, 7]. In both cases the values of the average path length and clustering coefficient are in accordance with expected small-world properties [6, 7].

Each node in our brain model is described by the Rulkov model [23], a discrete time system with two dimensions. The low-dimensionality of this map allow us to study large neural networks of approximately 10,000 neurons. This model has been extensively tested and it reproduces well the main features of realistic neural models. It has been used in studies about control of bursting synchronisation [24], phase synchronisation in clustered networks [16], and suppression of bursting synchronisation [25].

Our main goal is to show that pattern formation and collective behaviour in the brain might be a process mediated by other brain areas under stimulation. We also show that external perturbations induce synchrony behaviour in cognitive areas of the cat cerebral cortex. Bursting synchronisation appears between neurons in the auditory region when an external perturbation is applied in another cognitive area. We consider perturbations that activate neurons in accordance with experimental results in that pulses of blue light are capable to induce neuronal spikes [26, 27].

This paper is organised as follows: in Section II we introduce the network of Rulkov neurons and the cat brain matrix. In Section III, we study the phase synchronisation of the cognitive areas according to electrical and chem-

ical synapses. In Section IV, we analyse the effect of an external perturbation on the synchronisation. In the last Section, we draw the conclusions.

## 2. Network of Rulkov neurons

There is a wide range of mathematical models used to describe neuronal activity [23, 28, 29, 30]. In this work we consider the phenomenological model proposed by Rulkov

$$x_{n+1} = \frac{\alpha}{1 + x_n^2} + y_n, \quad (1)$$

$$y_{n+1} = y_n - \sigma(x_n - \rho), \quad (2)$$

where  $x_n$  and  $y_n$  are the fast and slow dynamical variables, respectively. The parameter  $\alpha$  affects the spiking time-scale, and we choose values in that the time series of  $x_n$  presents an irregular sequence of spikes. The parameters  $\sigma$  and  $\rho$  describe the slow time-scale. Figure 1 shows the time evolution of the fast and slow variables, where  $n_k$  is used to denote when neuronal bursting starts.

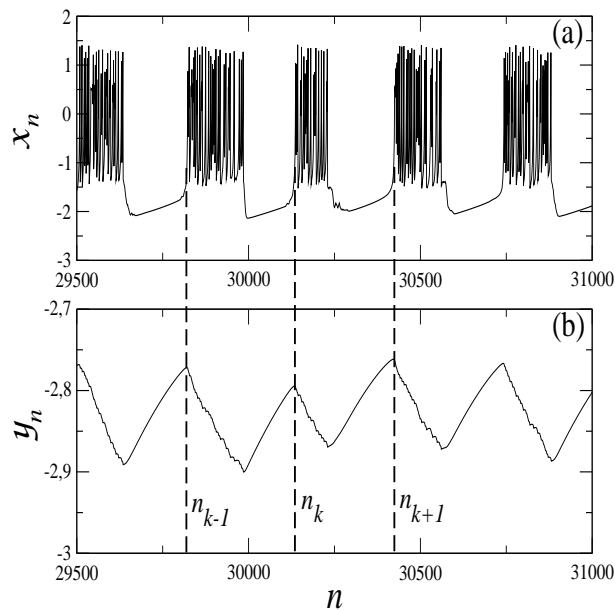


Figure 1: Time evolution of the (a) fast and (b) slow variables in the Rulkov map.

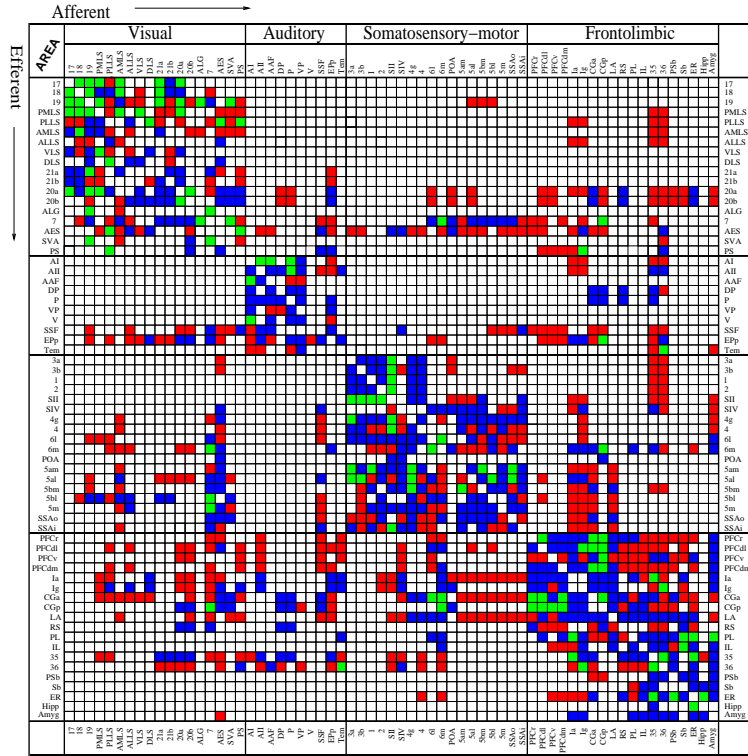


Figure 2: (Colour online) Density of connections between cortical areas classified as absent of connection (white), sparse (red), intermediate (blue), and dense (green).

We build a neuronal network considering the organisation of corticocortical connections obtained by Scannell and collaborators [7, 6, 8]. Figure 2 exhibits the matrix description of the corticocortical connectivity of the brain in accordance with Ref. [8]. In this work, the matrix elements have connections weighted 0, 1, 2, or 3, where 0 represents the absence of a connection between two brain areas, 1 represents a sparse connection, 2 represents an intermediate connection, and 3 is dense connections. In Figure 2 the colours are representing the weights white for no connections, sparse connections in red, intermediate connections in blue, and dense connections in green. All areas are grouped into 4 cognitive regions: visual, auditory, somatosensory-motor, and frontolimbic. The visual region has 18 cortical areas, the auditory has 10 areas, the somatosensory-motor has 18 areas, and the frontolimbic has 19 cortical areas.

The cortical areas contain a characteristic distribution of neuronal cells

and connections. Supporting evidences that there are small world properties at different level models of the brain [31, 32] we consider each cortical area as a small world network. A small-world has an average distance among neurons like a random network, while the degree of clustering is comparable to a regular network [14]. A small-world network has typically an average distance between sites comparable to the value it would take on for a random network, while retaining an appreciable degree of clustering, as in regular networks. Watts and Strogatz obtained small-world networks from an otherwise regular lattice with local connections, to which non local connections were added by randomly rewiring a small fraction of the local connections [14]. An alternative procedure was proposed by Newman and Watts, who inserted randomly chosen shortcuts in a regular lattice, instead of re-wiring local links into non-local ones [33]. We build small-world networks according to the procedure proposed by Newman and Watts. Each small-world network has 100 neurons and %5 of shortcuts. The connections among the small-world networks obey the corticocortical connectivity of the cat (Fig. 2) so that 2 areas connected with weight equal to 1 (red) have 50 randomly connections, areas connected with weight equal to 2 (blue) have 100 randomly connections, and areas with weight 3 (green) have 150 connections.

The coupling between neurons happens by means of electrical or chemical synapses. The local connections between neurons within each small-world network are described by electrical synapses. The shortcut non-local connections between neurons within each small-world network and the connections among cortical areas are described by chemical synapses. Chemical synapses may be excitatory or inhibitory. We consider that 75% are excitatory and 25% are inhibitory [34].

The dynamic behaviour of the neuronal network with electrical and chemical connections is governed by the following equations

$$x_{n+1}^{(i,p)} = \frac{\alpha^{(i,p)}}{1 + (x_n^{(i,p)})^2} + y_n^{(i,p)} + \frac{g_e}{\gamma^{(i,p)}} \sum_{\substack{(q,i) \in S \\ p \in P}} E_{(q,p),(i,p)} (x_n^{(q,p)} - x_n^{(i,p)}) - g_c \sum_{\substack{(d,i) \in S \\ (f,p) \in P}} [A_{(d,f),(i,p)} H(x_n^{(d,f)} - \theta) (x_n^{(i,p)} - V_s)] + \Lambda_n, \quad (3)$$

$$y_{n+1}^{(i,p)} = y_n^{(i,p)} - \sigma(x_n^{(i,p)} - \rho), \quad (4)$$

where  $S$  ( $i = 1, 2, \dots, S$ ) is the total number of neurons in each small-world,  $P$  ( $p = 1, 2, \dots, P$ ) is the number of cortical areas ( $P = 65$  according to Fig.

2),  $g_e$  is the electrical coupling strength,  $g_c$  is the chemical coupling strength,  $\alpha^{(i,p)}$  is the non-linearity parameter of the Rulkov map with values randomly coupled in the interval  $[4.1, 4.4]$ ,  $\sigma = 0.001$ , and  $\rho = -1.25$ . The term  $\Lambda_n$  is an external excitatory perturbation which activates spikes in randomly chosen neurons. The adjacency matrices  $E_{(q,p),(i,p)}$  and  $A_{(d,f),(i,p)}$  are the electric and chemical connections, respectively. They have elements with value equal to 1 when neuron  $(q, p)$  connects electrically with neuron  $(i, p)$ , and neuron  $(d, f)$  connects chemically with neuron  $(i, p)$ .  $H(x)$  is the Heaviside step function, where  $\theta = -1.0$  is the presynaptic threshold for the chemical synapse. When the presynaptic neuron voltage is above  $\theta$ , the postsynaptic neuron receives an input. This way,  $\theta$  is related to the sharp voltage response of the presynaptic terminals. The constant  $V_s$  denotes the reversal potential associated with the synapse, that is defined by the nature of the postsynaptic ionic channels. The synapse will be excitatory if  $V_s$  is higher and inhibitory if  $V_s$  is lower than a specific range [35]. Regarding the network of Rulkov neurons, for excitatory synapses  $V_s = 1.0$  and for inhibitory  $V_s = -2.0$ .

### 3. Burst synchronisation without external perturbation

Bursts of spikes and oscillatory patterns of neuronal activity have been observed in the central nervous system, ranging from slow to fast oscillations [36]. In fact, synchronised bursting has been verified in EEG recording of electrical brain activity. A type of synchronisation is the burst phase synchronisation [37].

Burst phase synchronisation is studied through the definition of a phase for neuronal bursting, defined by the slow variable. We consider that a burst begins when the slow variable  $y_n$ , shown in Fig. 1(b), has a local maximum happening in a time  $n_k$ . The duration of the burst,  $n_{k+1} - n_k$ , depends on the variable  $x_n$  and fluctuates in an irregular behaviour as long as  $x_n$  undergoes irregular evolution. Then, we define a phase describing the time evolution within each burst, varying from 0 to  $2\pi$  as  $n$  evolves from  $n_k$  to  $n_{k+1}$ ,

$$\phi_n = 2\pi k + 2\pi \frac{n - n_k}{n_{k+1} - n_k}, \quad (5)$$

where  $k$  is an integer.

We use the Kuramoto's order parameter as a diagnostic of the burst phase

synchronisation, that is defined as

$$z_n^{(l)} = R_n^{(l)} \exp(i\Phi_n^{(l)}) \equiv \frac{1}{N_l} \sum_{j \in I_l} \exp(i\phi_n^{(j, I_l)}), \quad (6)$$

where  $R_n$  is the amplitude and  $\Phi_n$  is the angle of a centroid phase vector for an one-dimensional network with periodic boundary conditions.  $I_l$  represents one of the four cognitive areas,  $l = 1$  for visual,  $l = 2$  for auditory,  $l = 3$  for somatosensory-motor, and  $l = 4$  for frontolimbic.  $N_l$  is the number of neurons of each area.  $\phi_n^{j, I_l}$  represents the phase of the neurons  $j$  belonging to the cortical area  $I_l$ . If the bursting phases  $\phi_n^{(j, I_l)}$  are uncorrelated, the summation in Eq. (6) is small and  $R_n^{(l)} \ll 1$ . Whereas  $R_n^{(l)} = 1$  when the cortical network area is in a completely burst phase synchronised state.

We are interested in studying the role of the electrical and chemical coupling strength at the level of bursting synchronisation. For this reason, we use the time averaged order parameter magnitude, given by

$$\bar{R}^{(l)} = \frac{1}{T} \sum_{n=1}^T R_n^{(l)}, \quad (7)$$

where  $T$  is the time interval, as a measure of synchronisation in the network. If the bursting dynamics in the area  $I_l$  is globally synchronised, we obtain  $\bar{R}^{(l)} \approx 1$ .

Figure 3 shows the time averaged order parameter in colour scale as a function of the electrical and chemical coupling strength. Due to the fact that the neurons are not identical the neuronal network does not present a completely phase synchronised state ( $\bar{R}^{(l)} \approx 1$ ). However, the network exhibits strong synchronisation for  $\bar{R}^{(l)} > 0.9$ , corresponding to the white region. All the cognitive areas, except for the auditory, present strong synchronisation (white region).

The auditory region does not present high levels of bursting synchronisation. This effect is due to the complex network topology, where the synchronisation patterns are controlled by input intensities among neurons, and also among the corticocortical areas [15]. To show that we define the mean field of the auditory area

$$M_n^{(2)} = \frac{1}{N_2} \sum_{(i, p) \in I_2} x_n^{(i, p)}, \quad (8)$$

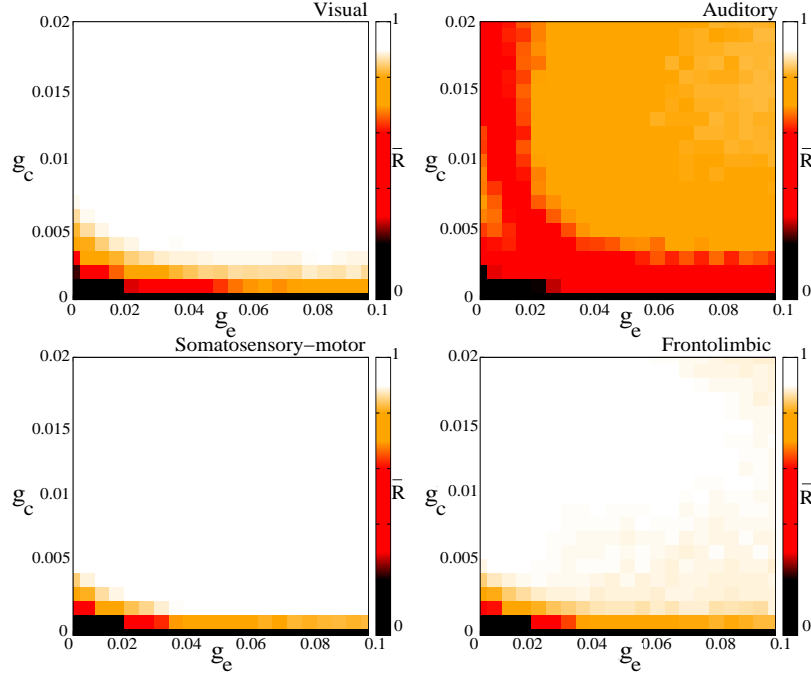


Figure 3: (Colour online) Average order parameter of the cat's cognitive brain regions. We consider 50000 iterations where 20000 were transient.

and the mean field of the  $N_{\text{out}}$  inputs coming from other areas

$$C_n^{(l)} = \frac{\mathfrak{S}_n^{(l)}}{N_{\text{out}}}, \quad (9)$$

where

$$\mathfrak{S}_n^{(l)} = -g_c \sum_{\substack{(i,p) \in I_2 \\ (d,f) \in I_1, I_2, I_3}} [A_{(d,f),(i,p)} H(x_n^{(d,f)} - \theta)(x_n^{(i,p)} - V_s)], \quad (10)$$

where  $N_{\text{out}}$  represents the number of non null elements in the matrix  $A_{(d,f),(i,p)}$  for  $(i,p) \in I_2$  and  $(d,f) \in I_1, I_2, I_3$ . We assume that each neuron  $(i,p)$  belonging to a set  $I_2$  in the auditory area is connected to a neuron  $(d,f)$  in a set  $I_l$  belonging to another cognitive area. Due to spatial distance between areas [38] we consider that the inputs from other areas are through chemical synapses [39].

Aiming to demonstrate that the absence of high levels of synchrony in the auditory area is an effect of the network, we compare the mean fields

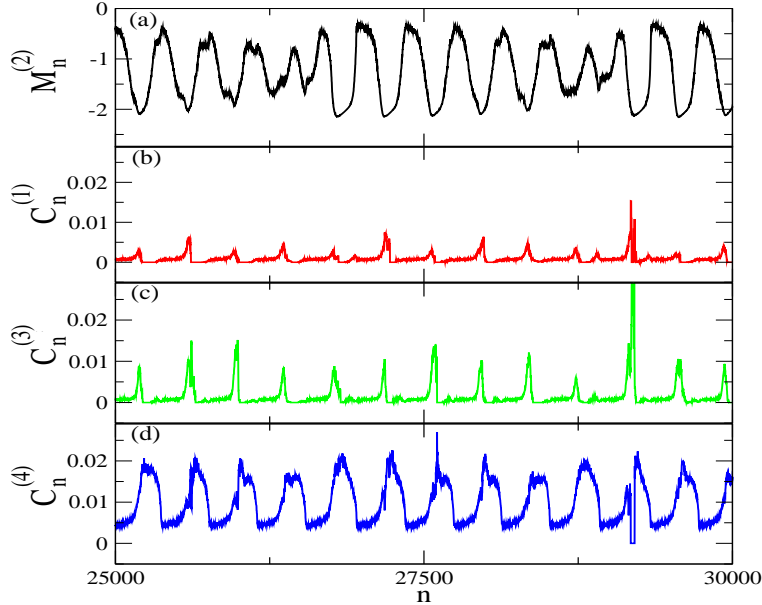


Figure 4: (Colour online) (a) Dynamics of the auditory fast variable mean field. Evolution of the external mean field on auditory area from (b) visual, (c) somatosensory-motor, and (d) frontolimbic areas. We consider  $g_e = 0.05$  and  $g_c = 0.015$ .

$M_n^{(2)}$  with  $C_n^{(1)}$ ,  $C_n^{(3)}$ , and  $C_n^{(4)}$ . Figure 4(a) exhibits the time evolution of the mean field  $M_n^{(2)}$  for  $N_2 = 1000$ . The irregular time evolution, that it is associated with a non synchronised behaviour, is influenced by the stimuli from the visual (Fig. 4b), the somatosensory-motor (Fig. 4c), and the frontolimbic (Fig. 4d) areas. This figure shows that the collective behaviour of the auditory area is correlated with the input from the frontolimbic. If the auditory area is isolated from other areas, by making  $A_{(d,f) \in I_1, I_3, I_4; (i,p)} = 0$  it will present global bursting synchronisation with a frequency around 0.0027. The frequency is obtained from bursts. Connecting the auditory area with the rest causes a suppression of bursting synchronisation, as well as the appearance of one more frequency with value equal to 0.0025 (Fig. 5a). We can see through Figure 5(b) that the new frequency appears by a resonant effect caused by the oscillations of the stimulus from others areas. The visual and somato-motor areas present the frequency equal to 0.0025 with magnitude equal to 0.0005 and 0.001, respectively. The frontolimbic area also exhibits this value of frequency, but the magnitude is larger than visual and somato-motor areas. Therefore, the low levels of synchrony in the auditory area is

mainly due to the new frequency of the input from frontolimbic area.

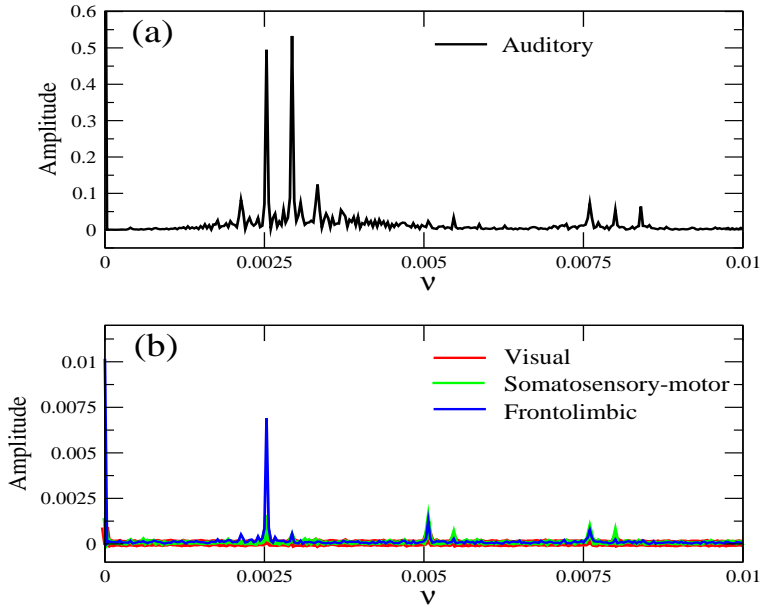


Figure 5: (Colour online) Frequencies of the (a) auditory fast variable mean field, and (b) external mean field on auditory area, considering  $g_e = 0.05$  and  $g_c = 0.015$ .

#### 4. External perturbation inducing synchronisation

It has been experimentally found that the incidence of light with a suitably chosen frequency on a group of neurons is able to alter their spiking activity. This phenomenon was verified by Boyden and collaborators [26, 27], by means of blue light they activated spikes in neurons genetically modified, and also suppressed spikes through yellow light. With this in mind, we consider an external perturbation ( $\Lambda_n$ ) acting on 100 neurons randomly chosen in the same cognitive area. This perturbation, aiming to simulate blue light optical stimulus, has excitatory effect on the perturbed neurons making them spike independent of their previous state.

We apply an external perturbation on the visual area to verify the synchronisation behaviour. Figure 6 shows the effects of this perturbation in the cognitive areas. Synchronisation is fully suppressed in the visual area. The somatosensory-motor and frontolimbic areas do not present significant alterations due to the perturbation in the visual area. This behaviour is due

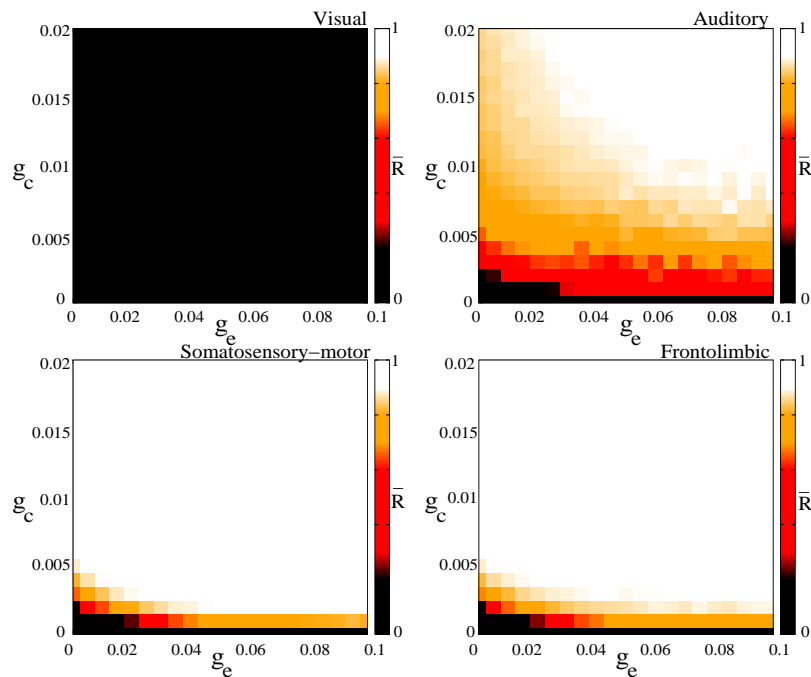


Figure 6: (Colour online) Order parameter of the cat's cognitive brain regions with an external perturbation on the visual area. We consider 50000 iterations, and 20000 transient iterations.

to the small number of connections between these areas and the visual area. On the other hand, the auditory area exhibits a change in its synchronous behaviour. Without an external perturbation the auditory area does not present high levels of synchronisation, shown in Figure 3, but with the perturbation in the visual area it is possible to observe strong synchronisation domains in the auditory area.

In order to understand the perturbation effect in the auditory area we calculate the time evolution of the mean field  $M_n^{(2)}$ , and the mean field from inputs coming from others areas  $C_n^{(1)}$ ,  $C_n^{(3)}$ , and  $C_n^{(4)}$  into the area  $I_2$ . Figure 7(a) shows that the mean field of the auditory area has a regular behaviour, whereas with no external perturbation the behaviour is irregular. Comparing the results of Figure 7 for the external inputs of the mean field on auditory from visual (b), somatosensory-motor (c), and frontolimbic (d) with the results of Figure 4 we can see that the inputs from the visual area becomes frequency-locked with the mean field  $M_n^{(2)}$  of the auditory area.  $M_n^{(2)}$  and

$C_n^{(1)}$  present both the same frequency, approximately 0.0028, as it can be seen in Fig. 8.

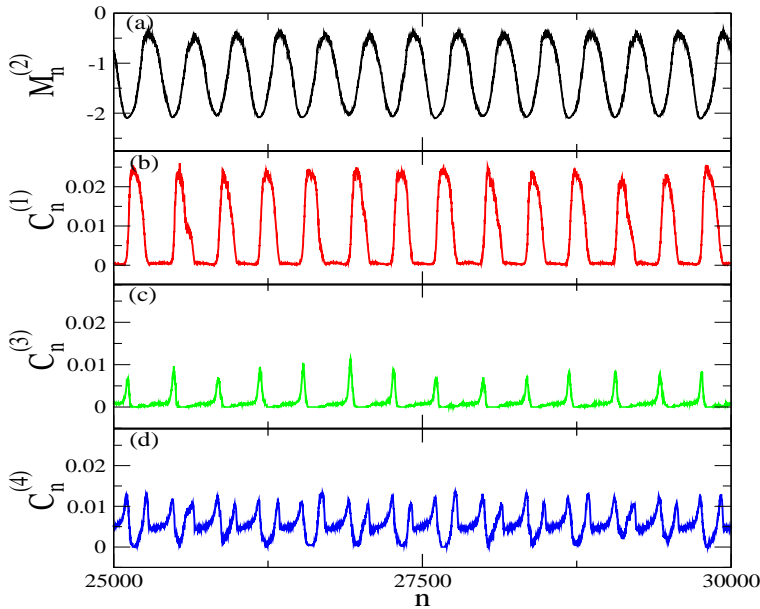


Figure 7: (Colour online) (a) Dynamics of the auditory fast variable mean field. Evolution of the external inputs mean field on the auditory area from (b) visual, (c) somatosensory-motor and (d) frontolimbic areas with an external perturbation on the visual area, considering  $g_e = 0.05$  and  $g_c = 0.015$ .

Perturbations applied in auditory area do not alter significantly the synchronous behaviour of the other areas. Moreover, we have verified which perturbations in the somatosensory-motor and frontolimbic areas produce the same effect on the network such as when they are applied in the visual area.

## 5. Conclusion

In this paper we studied burst phase synchronisation in a neuronal network with a topology according to the corticocortical connections of the cat cerebral cortex. When no perturbation is applied we verified that only the auditory area does not present synchronisation in the parameter space. This happens because of the large influence of the other areas. The ratio between inter connections and intra connections is less for the auditory area than

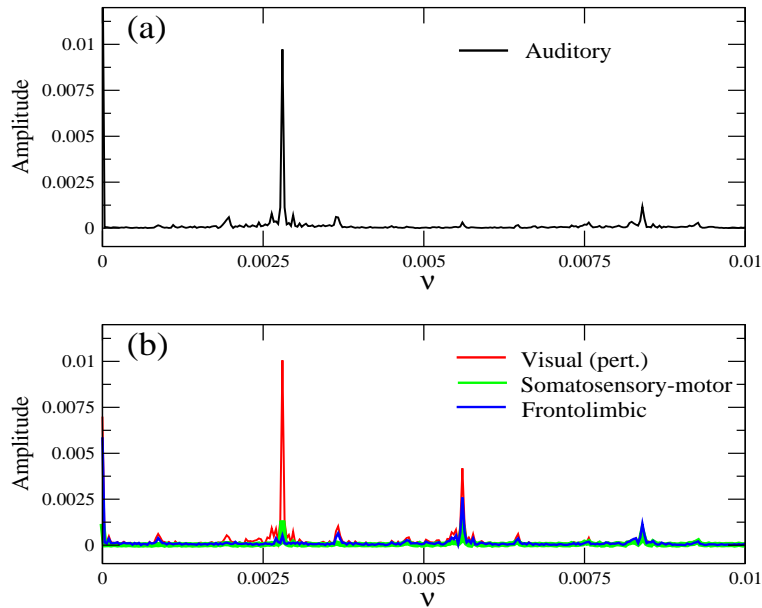


Figure 8: (Colour online) Frequencies of the (a) dynamics of the auditory fast variable mean field and (b) inputs mean field on auditory area for the system with external perturbation on visual area.

other areas. As the consequence the frontolimbic area induces a frequency in the auditory area which helps to suppress burst phase synchronisation.

We verified the suppression of burst phase synchronisation when a stimulus is applied on a cognitive area. However, the suppression in a specific area can affect another area. Our results have showed that an external perturbation applied into the visual area suppresses synchronisation in the visual area, but surprisingly it induces synchronisation in the auditory area. The same happens for perturbation applied in the somatosensory-motor and frontolimbic which induces synchronisation in the auditory area.

## Acknowledgements

This study was possible by partial financial support from the following Brazilian government agencies: CNPq, CAPES, Science Without Borders Program. Murilo S. Baptista also acknowledges EPSRC-EP/I032606/1.

## References

- [1] Koch C, Segev I. The role of single neurons in information processing. *Nature Neurosci* 2000;3:1171-1177.
- [2] Lent R, Azevedo FAC, Andrade-Moraes CH, Pinto AVO. How many neurons do you have? Some dogmas of quantitative neuroscience under revision. *E J Neurosci* 2012;35:1-9.
- [3] Bullmore E, Sporns O. Complex brain networks: graph theoretical analysis of structural and functional systems. *Nature Rev Neurosci* 2009;10:186-198.
- [4] Rockel AJ, Hiorns RW, Powell TPS. The basic uniformity in structure of the neocortex. *Brain* 1980;103:221-244.
- [5] Roland PE, Zilles K. Structural divisions and functional fields in the human cerebral cortex. *Brain Res Rev* 1998;26:87-105.
- [6] Scannell JW, Blakemore C, Young MP. Analysis of connectivity in the cat cerebral cortex. *J Neurosci* 1995;15:1463-1483.
- [7] Scannell JW, Young MP. The connectional organization of neural systems in the cat cerebral cortex. *Curr Biol* 1993;3:191-200.
- [8] Scannell JW, Burns GAPC, Hilgetag CC, O'Neil MA, Young MP. The connectional organization of the cortico-thalamic system of the cat. *Cereb Cortex* 1999;9:277-299.
- [9] Tonnelier A, Meignen S, Bosch H, Demongeot J. Synchronization and desynchronization of neural oscillators. *Neural Netw* 1999;12:1213-1228.
- [10] Lestienne R. Spike timing, synchronization and information processing on the sensory side of the central nervous system. *Prog Neurobiol* 2001;65:545-591.
- [11] Boucetta S, Chauvette S, Bazhenov M, Timofeev I. Focal generation of paroxysmal fast runs during electrographic seizures. *Epilepsia* 2008;49:1925-1940.

- [12] Schwab BC, Heida T, Zhao Y, Marani E, van Gils SA, van Wezel RJA. Synchrony in Parkinson’s disease: importance of intrinsic properties of the external globus pallidus. *Front Syst Neurosci* 2013;7:60.
- [13] Watts DJ. *Small Worlds*. Princeton University Press: Princeton; 2011.
- [14] Watts DJ, Strogatz SH. Collective dynamics of small-world networks. *Nature* 1998;393:440-442.
- [15] Zhou C, Zemanová L, Zamora-López G, Hilgetag CC, Kurths J. *New J Phys* 2007;9:178.
- [16] Batista CAS, Lameu EL, Batista AM, Lopes SR, Pereira T, Zamora-López G, Kurths J, Viana RL. Phase synchronization of bursting neurons in clustered small-world networks. *Phys Rev E* 2012;86:016211.
- [17] Korenkevych D, Chien J-H, Zhang J, Shiau D-S, Sackellares C, Pardalos PM. Small world networks in computational neuroscience. *Hand Comb Optim* 2013:3057-3088.
- [18] Varshney LR, Chen BL, Paniagua E, Hall DH, Chklovskii DB. Structural properties of the *Caenorhabditis elegans* neuronal network. *PLoS Comput Biol* 2011;7:e1001066.
- [19] He Y, Chen ZJ, Evans AC. Small-world anatomical networks in the human brain revealed by cortical thickness from MRI. *Cereb Cortex* 2007;17:2407-2419.
- [20] Stam CJ, Jones BF, Nolte G, Breakspear M, Scheltens P. Small-world networks and functional connectivity in Alzheimer’s disease. *Cereb Cortex* 2007;17:92-99.
- [21] Hilgetag CC, Kaiser M. Organization and function of complex cortical networks, *in* “Lectures in Supercomputational Neuroscience (Dynamics in Complex Brain Networks)”, Eds. Graben PB, Zhou C, Thiel M, Kurths J. Springer: Berlin-Heidelberg-New York; 2008.
- [22] Zamora-López G, Zhou C, Kurths J. Exploring brain function from anatomical connectivity. *Front Neurosci* 2011;5:83.
- [23] Rulkov NF. Regularization of synchronized chaotic bursts. *Phys Rev Lett* 2001;86:183-186.

- [24] Batista CAS, Lopes SR, Viana RL, Batista, AM. Delayed feedback control of bursting synchronization in a scale-free network. *Neural Net* 2010;23:114-124.
- [25] Lameu EL, Batista CAS, Batista AM, Iarosz KC, Viana RL, Lopes SR, Kurths J. Suppression of bursting synchronization in clustered scale-free (“rich-club”) neuronal networks. *Chaos* 2012;22:043149.
- [26] Han X, Boyden ES (2007). Multiple-color optical activation, silencing, and desynchronization of neural activity, with single-spike temporal resolution. *PLoS ONE* 2007;2:e299.
- [27] Boyden ES, Zhang F, Bamberg E, Nagel G, Deisseroth K. Millisecond-timescale, genetically targeted optical control of neural activity. *Nature Neurosci* 2005;8:1263-1268.
- [28] Hodgkin AL, Huxley AF. A quantitative description of membrane current and its application to conduction and excitation in nerve. *J Physiol* 1952;117:500-544.
- [29] Richard F. Mathematical models of threshold phenomena in the nerve membrane. *Bull Math Biophys* 1955;17:257-278.
- [30] Hindmarsh LJ, Rose RM. A model of neuronal bursting using three coupled first order differential equations. *Proc R Soc Lond B* 1984;221:87-102.
- [31] Sporns O, Chialvo DR, Kaiser M, Hilgetag CC. Organization, development and function in complex brain networks. *Trends Cogn Sci* 2004;8:418-425.
- [32] Shan Y, Huang D, Singer W, Nikolic D. A small world of neuronal Synchrony. *Cereb Cortex* 2008;18:2891-2901.
- [33] Newman MEJ, Watts DJ. Renormalization group analysis of the small-world network model. *Phys Lett A* 1999;263:341-346.
- [34] Bannister AP. Inter- and intra-laminar connections of pyramidal cells in the neocortex. *Neurosci Res* 2005;53:95-103.
- [35] Ibarz B, Casado JM, Sanjuán MAF. Map-based models in neuronal dynamics. *Phys Rep* 2011;501:1-74.

- [36] Buzsaki G. Rhythms of the brains. Oxford University Press: Oxford; 2006.
- [37] Batista CAS, Batista AM, Pontes JAC, Viana RL, Lopes SR. Chaotic phase synchronization in scale-free networks of bursting neurons. *Phys Rev E* 2007;76:016218.
- [38] Beul SR, Grand S, Hilgetag CC. *Brain Struct Funct* 2014;DOI 10.1007/s00429-014-0849-y.
- [39] Pereda AE. Electrical synapses and their functional interactions with chemical synapses. *Nature Rev Neurosci* 2014;15:250-263.